



Measurement of the branching ratio of the decay $D^0 \rightarrow \pi^- \mu^+ \nu$ relative to $D^0 \rightarrow K^- \mu^+ \nu$

FOCUS Collaboration¹

J.M. Link^a, P.M. Yager^a, J.C. Anjos^b, I. Bediaga^b, C. Göbel^b, A.A. Machado^b,
J. Magnin^b, A. Massafferri^b, J.M. de Miranda^b, I.M. Pepe^b, E. Polycarpo^b,
A.C. dos Reis^b, S. Carrillo^c, E. Casimiro^c, E. Cuautle^c, A. Sánchez-Hernández^c,
C. Uribe^c, F. Vázquez^c, L. Agostino^d, L. Cinquini^d, J.P. Cumalat^d, B. O'Reilly^d,
I. Segoni^d, K. Stenson^d, J.N. Butler^e, H.W.K. Cheung^e, G. Chiodini^e, I. Gaines^e,
P.H. Garbincius^e, L.A. Garren^e, E. Gottschalk^e, P.H. Kasper^e, A.E. Kreymer^e,
R. Kutschke^e, M. Wang^e, L. Benussi^f, M. Bertani^f, S. Bianco^f, F.L. Fabbri^f, A. Zallo^f,
M. Reyes^g, C. Cawfield^h, D.Y. Kim^h, A. Rahimi^h, J. Wiss^h, R. Gardnerⁱ,
A. Kryemadhiⁱ, Y.S. Chung^j, J.S. Kang^j, B.R. Ko^j, J.W. Kwak^j, K.B. Lee^j, K. Cho^k,
H. Park^k, G. Alimonti¹, S. Barberis¹, M. Boschini¹, A. Cerutti¹, P. D'Angelo¹,
M. DiCorato¹, P. Dini¹, L. Edera¹, S. Erba¹, P. Inzani¹, F. Leveraro¹, S. Malvezzi¹,
D. Menasce¹, M. Mezzadri¹, L. Moroni¹, D. Pedrini¹, C. Pontoglio¹, F. Prelz¹,
M. Rovere¹, S. Sala¹, T.F. Davenport III^m, V. Arenaⁿ, G. Bocaⁿ, G. Bonomiⁿ,
G. Gianiniⁿ, G. Liguoriⁿ, D. Lopes Pegnaⁿ, M.M. Merloⁿ, D. Panteaⁿ, S.P. Rattiⁿ,
C. Riccardiⁿ, P. Vituloⁿ, H. Hernandez^o, A.M. Lopez^o, H. Mendez^o, A. Paris^o,
J. Quinones^o, J.E. Ramirez^o, Y. Zhang^o, J.R. Wilson^p, T. Handler^q, R. Mitchell^q,
D. Engh^r, M. Hosack^r, W.E. Johns^r, E. Luiggi^r, J.E. Moore^r, M. Nehring^r,
P.D. Sheldon^r, E.W. Vaandering^r, M. Webster^r, M. Sheaff^s

^a University of California, Davis, CA 95616, USA

^b Centro Brasileiro de Pesquisas Físicas, Rio de Janeiro, RJ, Brazil

^c CINVESTAV, 07000 México City, DF, Mexico

^d University of Colorado, Boulder, CO 80309, USA

^e Fermi National Accelerator Laboratory, Batavia, IL 60510, USA

^f Laboratori Nazionali di Frascati dell'INFN, I-00044 Frascati, Italy

^g University of Guanajuato, 37150 Leon, Guanajuato, Mexico

^h University of Illinois, Urbana-Champaign, IL 61801, USA

ⁱ Indiana University, Bloomington, IN 47405, USA

^j Korea University, Seoul 136-701, South Korea

^k Kyungpook National University, Taegu 702-701, South Korea

¹ INFN and University of Milano, Milano, Italy^m University of North Carolina, Asheville, NC 28804, USAⁿ Dipartimento di Fisica Nucleare e Teorica and INFN, Pavia, Italy^o University of Puerto Rico, Mayaguez, PR 00681, USA^p University of South Carolina, Columbia, SC 29208, USA^q University of Tennessee, Knoxville, TN 37996, USA^r Vanderbilt University, Nashville, TN 37235, USA^s University of Wisconsin, Madison, WI 53706, USA

Received 26 October 2004; accepted 17 December 2004

Available online 29 December 2004

Editor: M. Doser

Abstract

We present a new measurement of the branching ratio of the Cabibbo suppressed decay $D^0 \rightarrow \pi^- \mu^+ \nu$ relative to the Cabibbo favored decay $D^0 \rightarrow K^- \mu^+ \nu$ and an improved measurement of the ratio $|f_+^\pi(0)/f_+^K(0)|$. Our results are $0.074 \pm 0.008 \pm 0.007$ for the branching ratio and $0.85 \pm 0.04 \pm 0.04 \pm 0.01$ for the form factor ratio, respectively.

© 2004 Elsevier B.V. Open access under [CC BY license](#).

1. Introduction

Semileptonic decays provide the advantage of having factorizable weak currents in the Hamiltonian which allows for a clean theoretical description. The hadronic current can be described in terms of two form factors, $f_+(q^2)$ and $f_-(q^2)$ which are functions only of the lepton–neutrino invariant mass squared, q^2 . Assuming a pole dominance parameterization of the form factors, we present a parametric analysis of the pseudoscalar semileptonic decays $D^0 \rightarrow \pi^- \mu^+ \nu$ and $D^0 \rightarrow K^- \mu^+ \nu$ from the FOCUS experiment.

This Letter concentrates on the relative branching ratio and the form factor ratio of the Cabibbo suppressed decay relative to the Cabibbo favored mode. Since the efficiency tends to have a non-negligible q^2 dependence (see [Fig. 3](#)), we allow the pole masses and the ratio $f_-(0)/f_+(0)$ to vary freely in the fit. The results and description of the detailed analysis of the pole masses and $f_-(0)/f_+(0)$ are included in another paper [\[1\]](#) along with a non-parametric analysis of the high statistics decay $D^0 \rightarrow K^- \mu^+ \nu$.

We report a new measurement for the branching ratio $\Gamma(\pi^- \mu^+ \nu)/\Gamma(K^- \mu^+ \nu)$ in agreement with re-

cent results from the CLEO Collaboration [\[2,3\]](#). These results indicate a lower value for this branching ratio than the one reported in the PDG [\[4\]](#). We also report a new measurement of the form factor ratio $|f_+^\pi(0)/f_+^K(0)|$ with greatly improved errors with respect to existing measurements and compare it to recent theoretical predictions from an unquenched Lattice QCD calculation [\[5,6\]](#).

2. Data selection

This analysis is based on data collected by the FOCUS experiment during the 1996–1997 fixed target run at Fermilab. FOCUS is a photoproduction experiment which collected a large sample of charm decays produced in the interactions of a photon beam [\[7\]](#) with an average energy of ~ 180 GeV on a BeO segmented target. The FOCUS spectrometer [\[8–11\]](#) is equipped with a 16 plane silicon strip vertex detector; 4 planes are interleaved with the targets and 12 planes are located downstream of the target area. Momentum analysis is accomplished by two magnets with opposite polarities and 5 multiwire proportional chambers. Three multi-cell threshold Čerenkov counters provide charged particle identification. A muon counter located at the end of the spectrometer is responsible for muon identification.

E-mail address: agostino@pizero.colorado.edu (L. Agostino).

¹ See <http://www-focus.fnal.gov/authors.html> for additional author information.

We reconstruct the semileptonic decays $D^0 \rightarrow \pi^- \mu^+ \nu$ and $D^0 \rightarrow K^- \mu^+ \nu$ requiring a D^{*+} -tag where the D^{*+} is reconstructed in the $D^0 \pi^+$ final state.² Whenever possible we apply identical selection criteria to both decay modes to reduce systematic effects. As the decay $D^0 \rightarrow \pi^- \mu^+ \nu$ has more background and less statistics, the selection cuts have been optimized for this mode. The signal and normalization samples are selected requiring two opposite charged tracks to form a good vertex with a confidence level greater than 1%. One of the two tracks from the D^0 decay vertex must be identified as a muon from the inner muon detector with a confidence level greater than 1% and must have momentum greater than 10 GeV/c. To suppress pion and kaon in-flight decays, this track is required to have a consistent momentum when measured in the first and second magnets. The other track must satisfy a Čerenkov requirement based on the value of the negative log-likelihood W for a given hypothesis: in the $D^0 \rightarrow \pi^- \mu^+ \nu$ mode, the pion must be favored with respect to the kaon hypothesis by at least 3 units of likelihoods ($W(K) - W(\pi) > 3$); in the case of $K^- \mu^+ \nu$ the kaon must be favored over the pion hypothesis by 3 units of likelihoods ($W(\pi) - W(K) > 3$). To reduce non-charm background, the candidate hadron must have a momentum greater than 14 GeV/c. The primary vertex is found after excluding the candidate tracks from the D^0 decay vertex; the remaining tracks are used to form candidate vertices. Of these vertices we choose the one with highest multiplicity and we break ambiguities by picking the most upstream vertex as the primary vertex. This vertex is required to be isolated from other tracks in the silicon strip vertex detector by requiring that the confidence level of any another track not used in the determination of the primary or decay vertex be less than 1%. For each hadron–lepton combination that satisfies the above requirements, another track coming from the primary vertex must be found as the candidate “soft” pion from the $D^{*+} \rightarrow D^0 \pi_s^+$. The π_s^+ candidate must not have the pion hypothesis strongly disfavored over all other particle hypotheses from the Čerenkov system ($\min\{W(e), W(K), W(p)\} - W(\pi) > -6$). It must also have a momentum greater than 2.5 GeV/c. To suppress backgrounds from decays where a final

state particle is lost (usually π^0), such as $K^- \pi^+ \pi^0$, $K^- \pi^+ \pi^0 \pi^0$, $\rho^- \mu^+ \nu$ and $K \pi \mu^+ \nu$,³ we place a lower cut on the hadron–lepton invariant mass (visible mass) of 1.0 GeV/c². Contamination from $D^0 \rightarrow K^- \pi^+$ is eliminated by requiring the visible mass to be less than 1.7 GeV/c².

Since the neutrino is not reconstructed, the resultant smearing effects on the resolution play an important factor in this analysis. Rather than using the standard neutrino closure resulting in a two-fold ambiguity on the D^0 momentum, we take advantage of the D^{*+} -tag by boosting the final state particles in the hadron–lepton center of mass frame. By constraining the $K^- \mu^+ \nu$ ($\pi^- \mu^+ \nu$) mass to the D^0 mass and the $K^- \mu^+ \nu \pi_s^+$ ($\pi^- \mu^+ \nu \pi_s^+$) mass to the D^{*+} mass, we are able to determine the angle between the neutrino⁴ and the π_s^+ direction. We then sample the azimuthal angle and choose the one that gives the direction of the D^0 most consistent with pointing to the primary vertex.

3. Analysis

The fit to the data is designed to constrain the background in the $\pi^- \mu^+ \nu$ sample and to supply information about the pole mass and form factors. To accomplish these goals we perform fits on two-dimensional distributions where the free parameters are the signal and background yields. All the fits are binned maximum likelihood fits where the likelihood is defined as

$$\mathcal{L} = \prod_{ij} \frac{f_{ij}^{n_{ij}} e^{-f_{ij}}}{n_{ij}!}, \quad (1)$$

where f_{ij} (n_{ij}) is the number of expected (observed) events in the bin ij . First, a fit of q^2 and $D^{*+} - D^0$ mass difference is performed to establish the amount of non-peaking background (Fig. 1).⁵ We next place a

³ With the notation $K \pi \mu^+ \nu$ we refer to the sum of the decays to $K^0 \pi^- \mu^+ \nu$ and $K^- \pi^0 \mu^+ \nu$ from D^0 or to the sum of the decays to $K^- \pi^+ \mu^+ \nu$ and $K^0 \pi^0 \mu^+ \nu$ from D^+ .

⁴ The neutrino and the D^0 directions are the same in this reference frame.

⁵ We define “peaking background” in the $\pi^- \mu^+ \nu$ sample as the sum of the background contributions from $D^0 \rightarrow K^- \mu^+ \nu$, $K \pi \mu^+ \nu$ and $\rho^- \mu^+ \nu$, while in the $K^- \mu^+ \nu$ sample the peaking background is given only by $K^- \pi^0 \mu^+ \nu$.

² Throughout this Letter charge conjugate modes are implied.

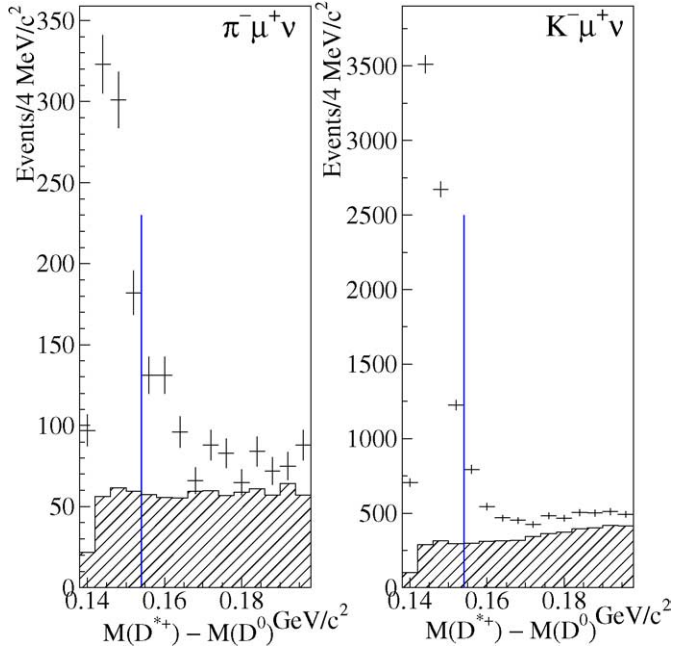


Fig. 1. $D^{*+}-D^0$ mass difference distributions for $D^0 \rightarrow \pi^- \mu^+ \nu$ (left) and $D^0 \rightarrow K^- \mu^+ \nu$ (right). The amount of non-peaking background is found from a fit to q^2 and $D^{*+}-D^0$ mass difference distributions. The vertical line indicates where the cut is placed.

mass cut on the $D^{*+}-D^0$ mass difference of less than $0.154 \text{ GeV}/c^2$ to reduce the background and to obtain more reliable results for parameters such as pole masses and form factors. A fit is then made to the two-dimensional distribution q^2 vs. $\cos \theta_\ell$ (where $\cos \theta_\ell$ is defined as the cosine of the angle between the neutrino direction and the D^0 direction in the rest frame of the lepton–neutrino system). The fit is first performed on the $K^- \mu^+ \nu$ sample and the results from this fit are used to set the background from $K^- \mu^+ \nu$ and $K \pi \mu^+ \nu$ in the $\pi^- \mu^+ \nu$ sample.

In the fit to the $K^- \mu^+ \nu$ distribution we make use of the recent vector to pseudoscalar branching ratio measurement $\Gamma(D^+ \rightarrow K \pi \mu^+ \nu)/\Gamma(D^+ \rightarrow \bar{K}^0 \mu^+ \nu) = 0.63 \pm 0.05$ [12] in the form of a penalty term added to the log-likelihood as shown in Eq. (2)

$$F_{K\mu\nu} = -2 \log \mathcal{L}_{K\mu\nu} + \frac{\left(\frac{Y_{K\pi\mu^+\nu} \epsilon(K^- \mu^+ \nu)}{Y_{K^- \mu^+ \nu} \epsilon(K\pi\mu^+\nu)} - 0.63 \right)^2}{(0.05)^2}, \quad (2)$$

where we assume isospin invariance to relate D^+ and D^0 decays. The likelihood \mathcal{L} is constructed using the

expected number of events in each ij bin of the two-dimensional distribution given by

$$f_{K^- \mu^+ \nu}^{ij} = Y_{K^- \mu^+ \nu} S_{K^- \mu^+ \nu}^{ij} + Y_{(c\bar{c})} S_{(c\bar{c})}^{ij} + Y_{K^- \pi^0 \mu^+ \nu} S_{K^- \pi^0 \mu^+ \nu}^{ij}, \quad (3)$$

where in Eqs. (2) and (3) the fit parameters Y_α are the fitted yields, S_α are the normalized shapes obtained from Monte Carlo and ϵ the reconstruction efficiency. We define the $c\bar{c}$ component as the background obtained from a high statistics charm–anticharm Monte Carlo sample after removing the modes handled specifically in Eq. (3) (and (5)).

In a similar way we fit the $\pi^- \mu^+ \nu$ distribution. We use the branching ratio $\Gamma(D^0 \rightarrow \rho^- \mu^+ \nu)/\Gamma(D^0 \rightarrow K \pi \mu^+ \nu) = 0.086 \pm 0.010^6$ to constrain the back-

⁶ We estimated the branching ratio of $D^0 \rightarrow \rho^- \mu^+ \nu$ relative to $D^0 \rightarrow K \pi \mu^+ \nu$ using the weighted average of a recent result from the CLEO-c Collaboration [3], the PDG values [4] and a preliminary result from FOCUS [13] where we correct for isospin when necessary.

ground in the fit as shown in Eq. (4)

$$F_{\pi\mu\nu} = -2 \log \mathcal{L}_{\pi\mu\nu} + \frac{\left(\frac{Y_{\rho^-\mu^+\nu}}{Y_{K\pi\mu^+\nu}} \frac{\epsilon(K\pi\mu^+\nu)}{\epsilon(\rho^-\mu^+\nu)} - 0.086 \right)^2}{(0.010)^2}. \quad (4)$$

The expected number of events in each two-dimensional bin used to construct the likelihood is

$$\begin{aligned} f_{\pi^-\mu^+\nu}^{ij} &= Y_{\pi^-\mu^+\nu} S_{\pi^-\mu^+\nu}^{ij} + Y_{(c\bar{c})} S_{(c\bar{c})}^{ij} \\ &+ Y_{\rho^-\mu^+\nu} S_{\rho^-\mu^+\nu}^{ij} \\ &+ Y_{K^-\mu^+\nu}^0 \frac{\epsilon((K^- \rightarrow \pi^-)\mu^+\nu)}{\epsilon(K^-\mu^+\nu)} \\ &\times S_{(K^- \rightarrow \pi^-)\mu^+\nu}^{ij} \\ &+ Y_{K^-\pi^0\mu^+\nu}^0 \frac{\epsilon((K^- \rightarrow \pi^-)\pi^0\mu^+\nu)}{\epsilon(K^-\pi^0\mu^+\nu)} \\ &\times S_{(K^- \rightarrow \pi^-)\pi^0\mu^+\nu}^{ij} \\ &+ 2Y_{K^-\pi^0\mu^+\nu}^0 \frac{\epsilon(K^0\pi^-\mu^+\nu)}{\epsilon(K^-\pi^0\mu^+\nu)} \\ &\times S_{K^0\pi^-\mu^+\nu}^{ij}, \end{aligned} \quad (5)$$

where $Y_{K^-\mu^+\nu}^0$ and $Y_{K^-\pi^0\mu^+\nu}^0$ in Eq. (5) are fixed to the results obtained from the fit to the $K^-\mu^+\nu$ data (Eq. (3)). The symbol $(X \rightarrow Y)$ means that a hadron X is misidentified as Y .

To measure pole masses and the form factor ratio $\eta \equiv f_-^K(0)/f_+^K(0)$ we apply an event-by-event weighting procedure [14]. This is achieved by reweighting each Monte Carlo event according to the ratio of the probability that the event was generated with a pole mass M'_{pole} and a form factor ratio η' relative to the probability that the event was generated with the default values $M_{D_s^*}$ (M_{D^*} for $\pi\mu\nu$) and η^0 .⁷ The relative efficiencies of the decays $D^0 \rightarrow \pi^-\mu^+\nu$ and $D^0 \rightarrow K^-\mu^+\nu$ are defined as the ratio of the reconstructed and generated Monte Carlo events. At each fit iteration these efficiencies change as a function of the pole masses and η values.

⁷ The default values for the parameter η are: $\eta^0 = -0.724$ for $D^0 \rightarrow K^-\mu^+\nu$ and $\eta^0 = -0.856$ for $D^0 \rightarrow \pi^-\mu^+\nu$.

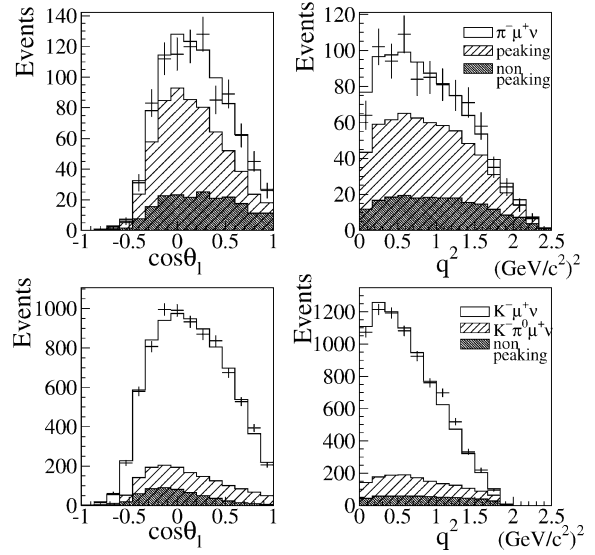


Fig. 2. Fit projections for $D^0 \rightarrow \pi^-\mu^+\nu$ and $D^0 \rightarrow K^-\mu^+\nu$. The fit is performed on a two-dimensional distribution of q^2 and $\cos\theta_\ell$. In the $D^0 \rightarrow \pi^-\mu^+\nu$, the peaking background contribution is defined as the sum of the contributions from $D^0 \rightarrow K^-\mu^+\nu$, $\rho^-\mu^+\nu$ and $K\pi\mu^+\nu$.

The weight W_i for an event with $q^2 = q_i^2$ is given by the equation

$$W_i = \frac{I(M'_{\text{pole}}, \eta'; q_i^2) N(M_{D_s^*}, \eta^0)}{I(M_{D_s^*}, \eta^0; q_i^2) N(M'_{\text{pole}}, \eta')}, \quad (6)$$

where the intensity is

$$I(M_{\text{pole}}, \eta; q^2) \propto f_+^2(M_{\text{pole}}; q^2) g(\eta) \quad (7)$$

and the normalization is determined by

$$N(M_{\text{pole}}, \eta) = \sum_{i=1}^{N_{\text{gen}}} f_+^2(M_{\text{pole}}; q_i^2) g(\eta). \quad (8)$$

The form factor $f_+(M_{\text{pole}}; q^2)$ is assumed to have the following q^2 dependence

$$f_+(M_{\text{pole}}; q^2) = \frac{f_+(0)}{1 - \frac{q^2}{M_{\text{pole}}^2}} \quad (9)$$

and $g(\eta)$ can be written in terms of three kinematic coefficients \mathcal{A} , \mathcal{B} and \mathcal{C} :⁸

$$g(\eta) = \mathcal{A} + \mathcal{B}\eta + \mathcal{C}\eta^2. \quad (10)$$

⁸ The kinematic dependence is shown in detail for kaon semileptonic decays in Ref. [4] on p. 618.

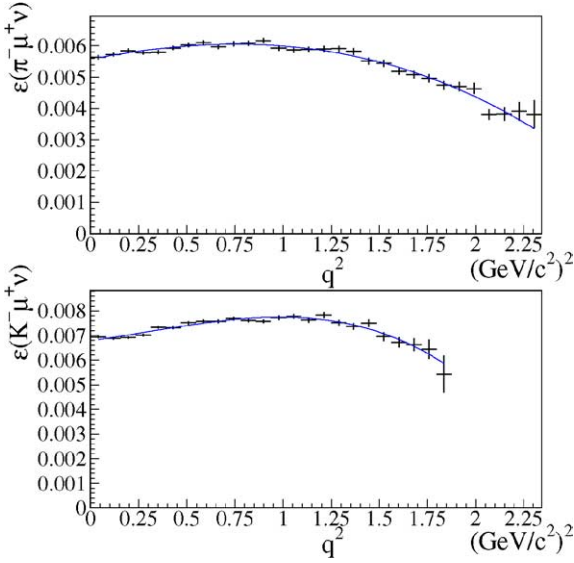


Fig. 3. Reconstruction efficiency as a function of the q^2 for $\pi^- \mu^+ \nu$ (top) and $K^- \mu^+ \nu$ (bottom).

From the fit to the $\pi^- \mu^+ \nu$ ($K^- \mu^+ \nu$) distributions (Fig. 2) we find 288 ± 29 $\pi^- \mu^+ \nu$ (6574 ± 92 $K^- \mu^+ \nu$) events. Correcting for the relative Monte Carlo efficiency we find the branching ratio for the Cabibbo suppressed decay $D^0 \rightarrow \pi^- \mu^+ \nu$ relative to the Cabibbo allowed decay $D^0 \rightarrow K^- \mu^+ \nu$ to be

$$\frac{\Gamma(D^0 \rightarrow \pi^- \mu^+ \nu)}{\Gamma(D^0 \rightarrow K^- \mu^+ \nu)} = 0.074 \pm 0.008(\text{stat.}). \quad (11)$$

From the same fits we find $M_\pi = 1.91^{+0.30}_{-0.15}$ GeV/c^2 and $M_K = 1.93^{+0.05}_{-0.04}$ GeV/c^2 for the $\pi^- \mu^+ \nu$ and the $K^- \mu^+ \nu$ pole masses, respectively. We also measure the ratio $f_-^K(0)/f_+^K(0) = -1.7^{+1.6}_{-1.4}$. A detailed description of the pole mass results has been included in Ref. [1].

Using the yields from the fit it is possible to obtain the ratio of the form factors $f_+^\pi(0)/f_+^K(0)$. In order to do this we compute a numerical integration of the differential decay rate modulated by the reconstruction efficiency as a function of the q^2 [15]. This efficiency is found by sampling the q^2 Monte Carlo distribution and dividing the reconstructed events by the generated events in each bin. The resultant distribution is then fit to a third degree polynomial (Fig. 3) which is used in the computation of the integral. We quote the result

$$\left| \frac{V_{cd}}{V_{cs}} \right|^2 \left| \frac{f_+^\pi(0)}{f_+^K(0)} \right|^2 = 0.037 \pm 0.004(\text{stat.}). \quad (12)$$

Applying the unitarity constraints on the CKM matrix elements [4] we use the value $|\frac{V_{cd}}{V_{cs}}|^2 = 0.051 \pm 0.001$ in Eq. (12) and measure the ratio $f_+^\pi(0)/f_+^K(0)$ to be

$$\left| \frac{f_+^\pi(0)}{f_+^K(0)} \right| = 0.85 \pm 0.04(\text{stat.}). \quad (13)$$

4. Systematic studies

Several studies have been performed to search for possible systematic uncertainties. The fitting procedure was tested on a Monte Carlo set whose size is roughly 20 times the FOCUS data set and we verified that the fit returned the input values used in our simulation.

We checked for possible biases as well as the accuracy of our statistical error by performing a fit on fluctuated data distributions multiple times and comparing the mean and width of the distribution of the fit results to our measurement. We found that we have to add a 0.005 contribution to the systematic error to compensate for $K^- \mu^+ \nu$ and $K \pi \mu^+ \nu$ contributions that were not allowed to float in the $\pi^- \mu^+ \nu$ fit. We also performed an analogous study using the fit function as the parent distribution to establish how well our fit function described the data. We compared the likelihood obtained from our measurement to the distribution of the likelihoods from the fluctuated fit function. We found good agreement indicating that our fit function well represents the data.

We investigated the stability of our results by changing a variety of selection criteria: the significance of separation between the primary and secondary vertex, muon identification, track momenta, visible mass cut, and Čerenkov identification. We found no significant change in our results and assign a systematic uncertainty of 0.003 on the branching ratio due to cut variations. This number is found by computing the variance of this set of results.

We further investigated fit variations by using a different approach in which we fit the q^2 and $D^{*+} - D^0$ mass difference. Rather than fitting the $K^- \mu^+ \nu$ distribution first, this fit was performed simultaneously on the $\pi^- \mu^+ \nu$ and $K^- \mu^+ \nu$ samples. The results are nearly identical to the results obtained from the fit to q^2 and $\cos \theta_\ell$. Other fit variations include changing the

Table 1

Sources of systematic errors and relative uncertainties. The contributions to the error on the ratio $f_+^\pi(0)/f_+^K(0)$ are found by propagating the corresponding errors on the branching ratio

	BR	$f_+^\pi(0)/f_+^K(0)$
Fluctuated data distribution	0.005	0.029
Cut variations	0.003	0.017
Fit variations	0.004	0.023
Čerenkov misidentification	0.002	0.011
Total	0.007	0.042

bin size. By computing the variance of these a priori likely results, we assigned a systematic uncertainty of 0.004 from fit variations.

Since the Monte Carlo is used to determine the amount of $K^-\mu^+\nu$ background in the $\pi^-\mu^+\nu$ sample, we are sensitive to the simulated misidentification rate. We used the high statistics modes $D^0 \rightarrow K^-\pi^+$ and $D^0 \rightarrow K^-\pi^+\pi^+$ where no Čerenkov requirement was applied to measure the $K \rightarrow \pi$ misidentification rate and we used the statistical error on the combined sample (after applying the same Čerenkov requirement used to select the $D^0 \rightarrow \pi^-\mu^+\nu$ events) to assign a systematic uncertainty. We varied the misidentification rate so obtained by $\pm 1\sigma$, and we find a contribution of 0.002 to the total systematic error.

The contributions to the systematic error on the branching ratio and the corresponding contributions to the error on the form factor ratio $f_+^\pi(0)/f_+^K(0)$ are listed in Table 1.

In the measurement of the form factor ratio $f_+^\pi(0)/f_+^K(0)$ we also added variations on the fit to the reconstruction efficiency as a function of the q^2 used in the numerical integration. We varied the bin size and fit functions. We find a contribution to the systematic error of 0.010 which is added in quadrature to the errors propagated from the branching ratio measurement.

5. Summary and conclusions

We quote the final results as

$$\frac{\Gamma(D^0 \rightarrow \pi^-\mu^+\nu)}{\Gamma(D^0 \rightarrow K^-\mu^+\nu)} = 0.074 \pm 0.008(\text{stat.}) \pm 0.007(\text{sys.}) \quad (14)$$

and

$$\left| \frac{V_{cd}}{V_{cs}} \right|^2 \left| \frac{f_+^\pi(0)}{f_+^K(0)} \right|^2 = 0.037 \pm 0.004(\text{stat.}) \pm 0.004(\text{sys.}) \quad (15)$$

Using $\left| \frac{V_{cd}}{V_{cs}} \right|^2 = 0.051 \pm 0.001$ from unitarity constraints, we find the form factor ratio to be

$$\left| \frac{f_+^\pi(0)}{f_+^K(0)} \right| = 0.85 \pm 0.04(\text{stat.}) \pm 0.04(\text{sys.}) \pm 0.01(\text{CKM}), \quad (16)$$

where the last error (CKM) corresponds to the uncertainty on the ratio $|V_{cd}/V_{cs}|$. We compare our results to the measurement reported by the CLEO Collaboration in Ref. [2] where they report the branching ratio of $D^0 \rightarrow \pi^-e^+\nu$ relative to $D^0 \rightarrow K^-e^+\nu$ to be $0.082 \pm 0.006 \pm 0.005$ and the form factor ratio $|f_+^\pi(0)/f_+^K(0)| = 0.86 \pm 0.07_{-0.04}^{+0.06} \pm 0.01$. We also compare our branching ratio result to the recent measurement from absolute branching ratios for $D^0 \rightarrow \pi^-e^+\nu$ and $D^0 \rightarrow K^-e^+\nu$ from CLEO-c [3] where they report a relative branching ratio of $0.070 \pm 0.007 \pm 0.003$. Our results are consistent with both of these new measurements. Further, we report an improved measurement of $|f_+^\pi(0)/f_+^K(0)|$ in good agreement with SU(3) breaking expected in recent lattice QCD calculations where they quote a form factor ratio value of 0.85 ± 0.05 [5] and $0.86 \pm 0.05 \pm 0.11$ [6].

Acknowledgements

We wish to acknowledge the assistance of the staffs of Fermi National Accelerator Laboratory, the INFN of Italy, and the physics departments of the collaborating institutions. This research was supported in part by the US National Science Foundation, the US Department of Energy, the Italian Istituto Nazionale di Fisica Nucleare and Ministero dell'Università e della Ricerca Scientifica e Tecnologica, the Brazilian Conselho Nacional de Desenvolvimento Científico e Tecnológico, CONACyT-México, the Korean Ministry of Education, and the Korean Science and Engineering Foundation.

References

- [1] FOCUS Collaboration, J.M. Link, et al., hep-ex/0410037.
- [2] CLEO Collaboration, G.S. Huang, et al., hep-ex/0407035.
- [3] CLEO Collaboration, K.Y. Gao, in: The 32nd International Conference on High Energy Physics, Beijing, August 2004, hep-ex/0408077.
- [4] Particle Data Group, S. Eidelman, et al., Phys. Lett. B 592 (2004) 1.
- [5] M. Okamoto, et al., Nucl. Phys. B (Proc. Suppl.) 129 (2004) 334.
- [6] Fermilab Lattice Collaboration, C. Aubin, et al., hep-ph/0408306.
- [7] E687 Collaboration, P.L. Frabetti, et al., Nucl. Instrum. Methods A 329 (1993) 62.
- [8] E687 Collaboration, P.L. Frabetti, et al., Nucl. Instrum. Methods A 320 (1992) 519.
- [9] FOCUS Collaboration, J.M. Link, et al., Nucl. Instrum. Methods A 516 (2004) 364.
- [10] FOCUS Collaboration, J.M. Link, et al., Phys. Lett. B 535 (2002) 43.
- [11] FOCUS Collaboration, J.M. Link, et al., Nucl. Instrum. Methods A 484 (2002) 270.
- [12] FOCUS Collaboration, J.M. Link, et al., Phys. Lett. B 598 (2004) 33.
- [13] FOCUS Collaboration, E. Luiggi, Analysis of $D^+ \rightarrow \rho^0 \mu^+ \nu$ in FOCUS, Talk presented at the Division of Particle and Fields Conference, 2004.
- [14] E687 Collaboration, P.L. Frabetti, et al., Phys. Lett. B 364 (1995) 127.
- [15] E687 Collaboration, P.L. Frabetti, et al., Phys. Lett. B 382 (1996) 312.